Creep Damage Assessment Considering Stress Multiaxiality for Notched Specimens of a CrMoV Steel

Nobuhiro ISOBE[1], Kenji YASHIRODAI[2] and Ken'ichi MURATA[2]

[1] Hitachi Research Laboratory, Hitachi, Ltd.
7-1-1, Oomika, Hitachi, Ibaraki 319-1292, Japan
E-mail: nobuhiro.isobe.jk@hitachi.com
[2] Thermal Power Systems, Power System Company, Hitachi, Ltd
3-1-1, Saiwai, Hitachi, Ibaraki 317-8511, Japan

ABSTRACT. *Creep damage assessment methods considering the effect of stress multiaxiality are discussed in order to evaluate creep crack initiation from stress concentrating fields such as notch roots. Creep tests using notched specimens were performed and damaging features around the notch root were investigated. Micro damages such as small creep cracks were mainly observed around several hundred micro-meters below the surface. Inelastic analyses taking primary creep into account were also performed. The area of high stress multiaxiality obtained from the analyses coincides with the area where micro damages were observed. Creep damage evaluation methods are also discussed. The strain based method was in good agreement with experimental results. Stress multiaxiality should be considered in evaluation of creep damage in stress concentrating fields.*

INTRODUCTION

Reliability against creep is an important factor in the design and life management of turbine components such as rotors and blades in high temperature stages. Uniaxial creep data is typically used when designing these components. The most severe portion from the viewpoint of material strength, however, is the stress concentrating area around the joint between the rotor and blades, which is where multiaxial stress states generate.

Materials used for these components usually have the notch strengthening property in creep. Stress multiaxiality at the stress concentrating area reduces creep rates and improves the rupture lives of the notched components of such materials [1, 2, 3]. Design based on uniaxial creep data, therefore, is a reasonable approach because it gives conservative evaluations. However, improving the life evaluation methods for these components taking the stress multiaxiality into account is important in terms of rationalizing the design and life management of turbines.

In this study, we performed creep tests and inelastic analyses of circumferentially notched bar specimens of a CrMoV steel for turbine rotors. Features of creep cracks were investigated and compared with stress and strain state obtained by inelastic

analyses. Evaluation methods of creep damage are also discussed by taking the stress multiaxiality into account.

EXPERIMENTAL PROCEDURES

The material employed in this study is a forged CrMoV steel for the turbine rotors. The shape and dimensions of the circumferentially notched bar specimens are shown in Fig. 1. Four notches are introduced ti the specimen. Diameters at the notch root are changed in order to investigate damaging features at each root. The minimum diameter is 8 mm and is increased by 0.05mm so that the maximum diameter is 8.15 mm. The radii of the curvatures at the notch root are 1.0 mm and 0.5 mm and stress concentration factors are 2.3 and 3.1 respectively.

Creep tests of the notched bar specimen were conducted in air at 575°C. A lever type creep test machine with an electric furnace was used. Testing loads were settled as nominal stress σ_n at minimum cross section of 400, 373, 350, 324 and 245 MPa.

Uniaxial creep tests using a smooth bar specimen were also perfomed for comparison.

TEST RESULTS

Creep Rupture Lives

The creep rupture lives of the notched and smooth bar specimens obtained in this study are shown in Fig. 2. For the notched specimens, the ordinate is nominal stress at the ruptured portion. The rupture lives of these specimens were longer than those of smooth bar specimens, which indicates that this steel exhibits notch strengthening property. The rupture lives of the smooth bar specimen can be approximated by two straight lines in a logarithm graph to divide the shorter and longer life regions. The dotted line in Fig. 2 is a 1.3 times translation of the trend in the longer life region of smooth bar specimen on the vertical axis. The difference between notch radius – 1.0 and 0.5 mm – is considered small in light of the test condition used in this study.

The minimum cross section was not always the failure location, especially in the specimen with 1.0-mm curvature radius, in which failure often occurred at the 8.10-mm diameter notch, which is the second largest cross section. The difference in cross section introduced in the specimen used in this study is regarded as included in the data scatter.

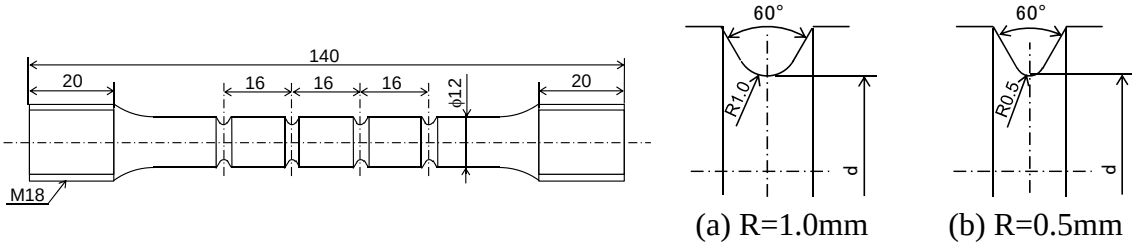

(a) R=1.0mm (b) R=0.5mm

Figure 1. Shape and dimension of notched specimens.

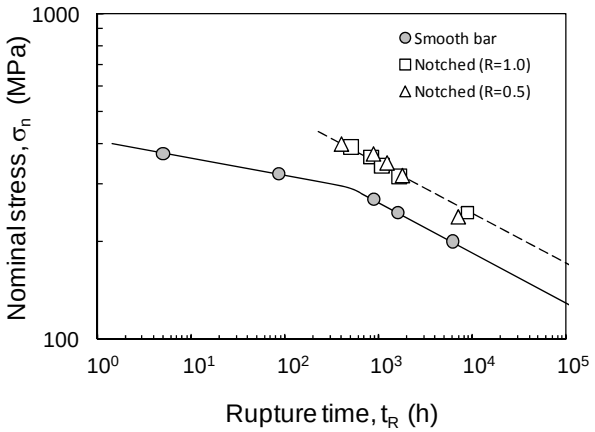

Figure 2. Nominal stress vs. creep rupture time.

Creep Cracking Features

Figure 3 shows SEM photographs of a cross section in the axial direction of several notched specimens. Inner cracks initiated at several hundred micro-meters from the notch root are mainly observed. Creep deformation is not obvious in these pictures, while in the smooth bar specimens, creep deformation dominates and creep crack can not be clearly observed. The damage mechanism of the two specimens might be different due to stress multiaxiality around the notch root. Creep deformation is suppressed by stress multiaxiality and cracking by void nucleation and their coalescence is considered the damage mechanism in the notched specimen even under higher stress conditions.

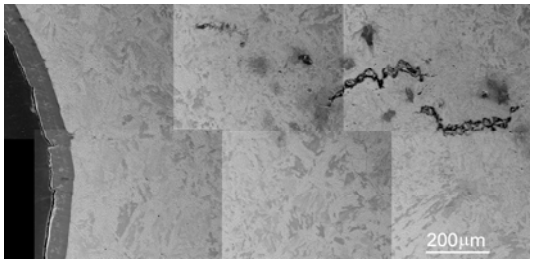

(a) R=1.0mm, σ_n=400MPa

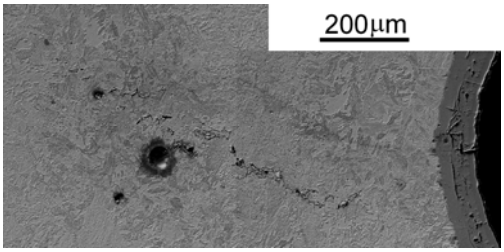

(b) R=0.5mm, σ_n=373MPa

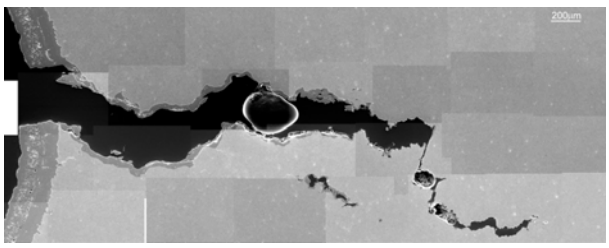

(c) R=1.0mm, σ_n=245MPa

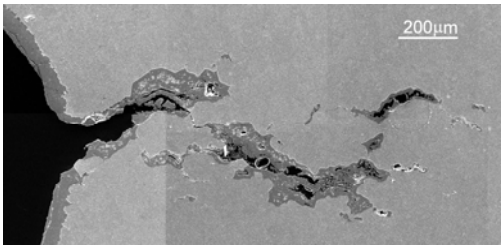

(d) R=0.5mm, σ_n=245MPa

Figure 3. Creep cracks observed in cross section of notched specimens.

CREEP DAMAGE ASSESSMENT

Inelastic Analyses

Inelastic analyses of the notched specimens were performed. A Blackburn-type creep equation derived from the creep curves of the smooth bar specimen was used in these analyses. The equation is expressed as,

$$\varepsilon_c = C_1\{1-\exp(-r_1 t)\} + \dot{\varepsilon}_m \cdot t\,, \tag{1}$$

$$r_1 = B_1 \cdot t_R^{\gamma_1}\,. \tag{2}$$

A comparison of the creep equation and experimental data (Fig.4) showed that the two were in good agreement in the primary and steady creep regions.

Figure 5 shows creep strain behaviors at the notch root obtained by creep analyses for test conditions of 400 and 245 MPa of the nominal stress. Chain lines in Fig. 5 represent the uniaxial creep curve by Eqs (1) and (2). The creep strain rate in the notched specimens is considerably reduced compared with uniaxial creep curve. Around

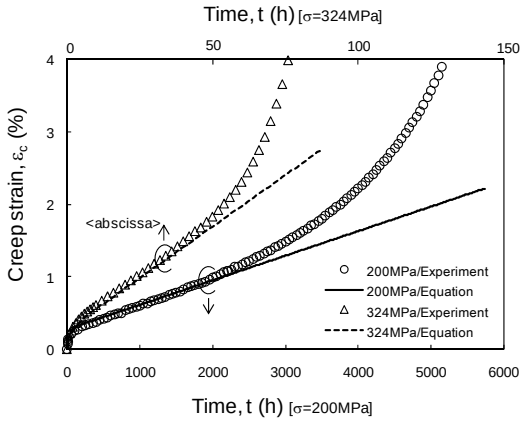

Figure 4. Comparison of creep strain equation with uniaxial creep test data.

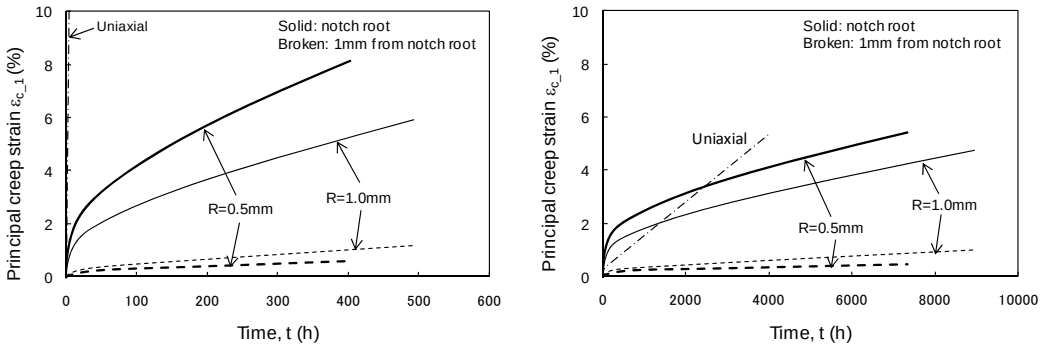

(a) σ_n=400MPa (b) σ_n=245MPa

Figure 5. Creep strain behavior obtained from inelastic analyses of notched specimens.

1 mm from the notch root surface, where the creep crack initiation is observed (Fig. 4), the creep strain is quite small: less than 1 % even at the time of rupture in the experiment.

The stress distributions in the cross section of notches for 245 MPa of the nominal stress condition are shown in Fig. 6. Principal stress, σ_1, is relatively larger than von Mises equivalent stress, σ_{eq}, because of the triaxial stress state. As for the principal stress, the position of its maximum moved to the inner side as time passed and settled at about 1 mm from the surface for 1-mm notch radius specimen and about 0.5 mm for 0.5-mm notch radius specimen at the middle of life. The maximum point of the equivalent stress remained at the surface all times.

Figure 7 shows the distributions of triaxiality factor, *TF*, which is expressed as,

$$TF = \frac{3\sigma_H}{\sigma_{eq}} = \frac{\sigma_1 + \sigma_2 + \sigma_3}{\frac{1}{\sqrt{2}}\left\{(\sigma_1 - \sigma_2)^2 + (\sigma_2 - \sigma_3)^2 + (\sigma_3 - \sigma_1)^2\right\}}, \tag{3}$$

where σ_H is the hydrostatic stress. *TF* is higher at the inner side than at the surface and the maximum point almost coincides with the maximum point of σ_1. These areas also agree with the creep cracking areas shown in Fig. 3. Stress multiaxiality is considered as an important factor contributing the creep damaging of the notched specimens, i.e., the stress concentrating field.

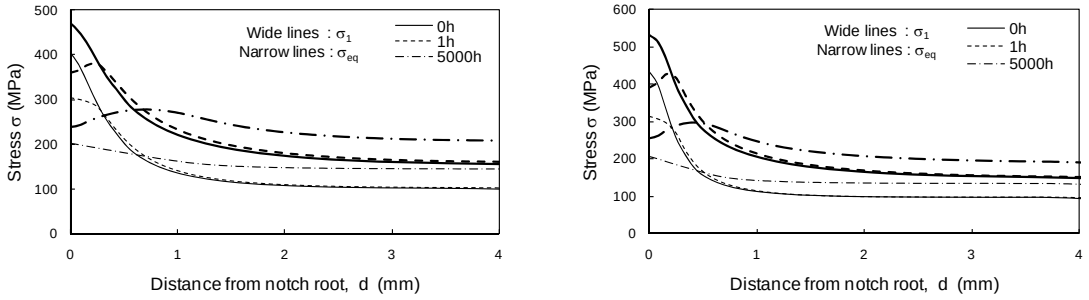

(a) R=1.0mm, σ_n=245MPa (b) R=0.5mm, σ_n=245MPa

Figure 6. Stress distribution in the cross section of notched specimens.

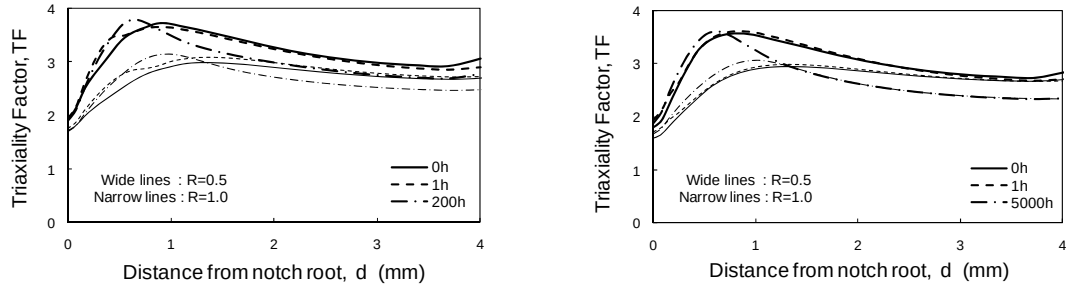

(a) σ_n=400MPa (b) σ_n=245MPa

Figure 7. Distribution of triaxiality factor in the cross section of notched specimens.

Creep Damage Assessment

The creep ductility of metals reduces under multiaxial stress states, and several models for evaluating creep ductility reduction have been proposed [4, 5]. The failure of notched specimens occurs though creep strains obtained from inelastic analyses are quite small, so ductility reduction due to stress multiaxiality might affect the creep damaging of notched specimens.

A model for ductility reduction under multiaxial stress state, previously introduced in R5 [6], used the following equation,

$$\frac{\varepsilon_f}{\varepsilon_{f0}} = \exp\left[p\left(1-\frac{\sigma_1}{\sigma_{eq}}\right)\right]\cdot\exp\left[q\left(\frac{1}{2}-\frac{3\sigma_H}{2\sigma_{eq}}\right)\right], \tag{4}$$

where σ_1, σ_H and σ_{eq} are the maximum principal, hydrostatic and von Mises equivalent stressess, respectively. ε_f is creep ductility and ε_{f0} is the ductility under the uniaxial stress condition. This model is used in order to evaluate the effect of stress multiaxiality in the assessment of creep damage in this study.

Creep damage evaluation methids by using stress and strain behaviors obtained from inelastic analyses are discussed. Two basic approaches are examined: the strain-based approach and the stress-based approach. The strain-based approach is similar to the ductility exhaustion concept. Creep damage D_c is calculated by

$$D_c = \int \frac{d\varepsilon_c}{\varepsilon_f\left(\sigma_1,\sigma_{eq},\sigma_H\right)}, \tag{5}$$

where ε_f is calculated by using eq. (4) and the effect of stress multiaxiality is considered as the reduction of creep ductility. Creep ductility under the uniaxial condition, ε_{f0}, is the basic parameter in this method, and its value is settled as 20 % according to the uniaxial creep test result conducted in this study.

In the stress-based approach, creep damage is evaluated by

$$D_c = \int \frac{dt}{t_R\left(\sigma\right)}, \tag{6}$$

where t_R is the rupture time. This approach coincides with the time fraction concept. The rupture curve of notched bar specimens, which is 1.3 times greater than that of the smooth bar specimens in the ordinate (Fig. 2) is used in this evaluation. Stress and strain behaviors obtained from inelastic analyses for notched bar specimens are introduced to Eqs (4) and (5) to evaluate creep damage.

Figures 8 and 9 show the creep damage distributions on a cross section of a notch portion at the time corresponding to the rupture in experiments under a test condition of 400 and 245 MPa. With the strain-based approach, creep damages is at a maximum several hundreds of micro-meters from the surface of the notch root (where the

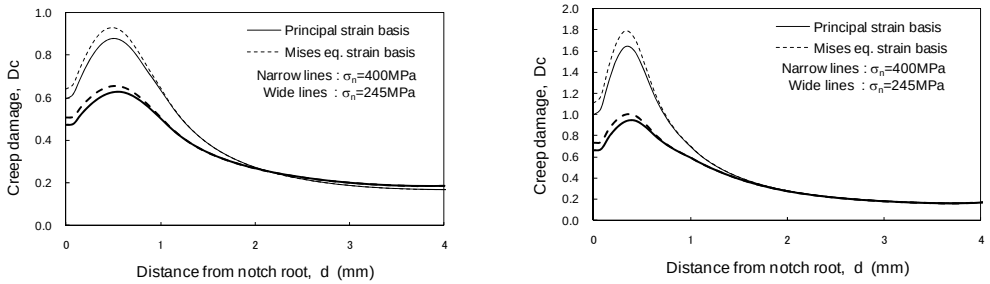

(a) R=1.0mm (b) R=0.5mm

Fig.8 Distribution of creep damage by the strain base method.

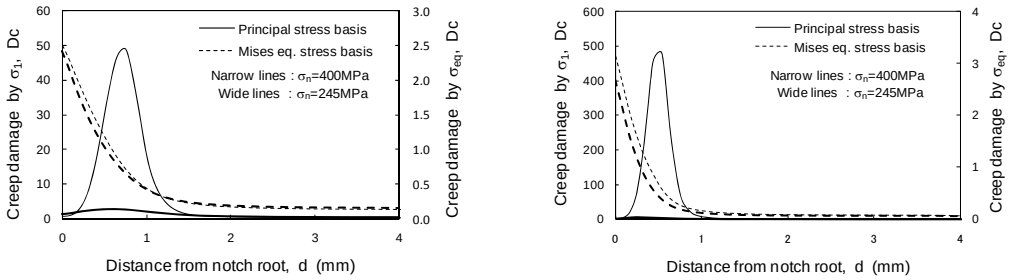

(a) R=1.0mm (b) R=0.5mm

Fig.9 Distribution of creep damage by the stress base method.

initiation of creep voids and cracks were observed in the experiment shown in Fig. 2), and their values are close to one. The difference of creep damage obtained by the principal strain to the von Mises equivalent strain is small. This means that the strain-based approach can provide reasonable results in creep damage assessment. In contrast, creep damage by the stress-based approach varies widely depending on the magnitude of stress and equivalent stress employed. Creep damage is at a maximum almost the same point as the strain-based approach when the principal strain is used for the creep damage evaluation, but this method has strong stress sensitivity, and the value of creep damage becomes too large under a large nominal stress condition: approximately 500 in the specimen with 0.5-mm notch radius under 400 MPa of nominal stress. Creep damages obtained by using von Mises equivalent stress is at a maximum at the surface, and the distribution of damage did not coincide with that of the creep void and crack observed in Fig. 3, even though the damage values are reasonably moderate.

A comparison of the strain- and stress-based approaches is summarized in Fig. 10, which shows the creep damages for all the tests carried out in this study. The stress dependency in the stress-based approach is extremely large compared with the strain-based approach. This means that creep damage evaluation using the stress based approach is not ideal for life assessment under the condition of high stress multiaxiality. The strain-based approach is a more suitable method, even though it also has stress dependency. In this study, ε_{f0} is settled as 20 % regardless of stress condition. Creep ductility usually reduces under the longer life condition, and the stress dependency in strain-based approach may be eliminated by introducing this effect.

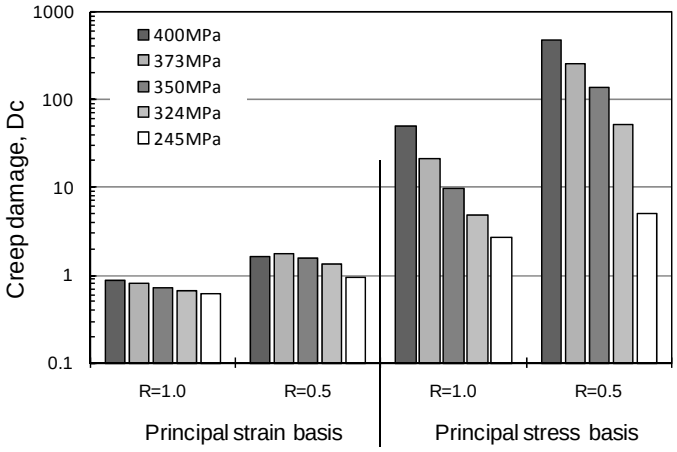

Fig.12 Comparison of creep damage obtained by strain- and stress-based methods for notched specimens.

SUMMARY

Creep damage assessment under the high stress multiaxiality condition was discussed using the creep test results of notched bar specimens. Creep damage by the strain-based approach, which features creep ductility reduction under the multiaxial stress condition, delivered a reasonable assessment result, whereas the stress-based approach overestimated the creep damage. It was also found that the distribution of damage obtained by the strain-based method was in good agreement with crack distribution observed in experiments. Stress multiaxiality is a key factor in creep damage and life evaluation in actual components.

REFERENCES

1. Takahashi, Y. (2009) *Journal of the Society of Materials Science, Japan,* **58**, 115–121, *in Japanese*.
2. Yoshida, K., Yatomi, M., Tanaka, Y., Kubushiro, K., Tabuchi, M. and Kobayashi, K. (2011) *Proceedings of the 49th Symposium on Strength of Materials at High Temperatures*, 57–61, *in Japanese.*
3. Sakurai, S., Fukuda, Y. and Kaneko, R. (1992) *Journal of the Society of Materials Science, Japan,* **41**, 1743–1748, *in Japanese.*
4. Cocks, A. C. F. and Ashby, M. F. (1980) *Metal Science*, 14, 395–402.
5. Rice, J. R. and Tracy, D. M. (1969), *Journal of the Mechanics and Physics of Solids,* 17, 201–217
6. British Energy (2003). *Assessment procedure for the high temperature response of structures*, *R5*, Issue 3